Advances in Water Resources 96 (2016) 120–126

Contents lists available at ScienceDirect

Advances in Water Resources

journal homepage: www.elsevier.com/locate/advwatres

Short communication

Does streambed heterogeneity matter for hyporheic residence time distribution in sand-bedded streams?

Daniele Tonina[a,*], Felipe P.J. de Barros[b], Alessandra Marzadri[a], Alberto Bellin[c]

[a] Center for Ecohydraulics Research, University of Idaho, Boise, USA
[b] Sonny Astani Department of Civil and Environmental Engineering, University of Southern California, Los Angeles, CA, USA
[c] Departement of Civil Enviromental and Mechanical Engineering, University of Trento, Trento. Italy

ARTICLE INFO

Article history:
Received 3 April 2016
Revised 15 July 2016
Accepted 16 July 2016
Available online 18 July 2016

Keywords:
Hyporheic flow
Heterogeneity
Bedforms
Greenhouse emissions

ABSTRACT

Stream water residence times within streambed sediments are key values to quantify hyporheic processes including sediment thermal regime, solute transient storage, dilution rates and biogeochemical transformations, such as those controlling degassing nitrous oxide. Heterogeneity of the streambed sediment hydraulic properties has been shown to be potentially an important factor to characterize hyporheic processes. Here, we quantify the importance of streambed heterogeneity on residence times of dune-like bedform induced hyporheic fluxes at the bedform and reach scales. We show that heterogeneity has a net effect of compression of the hyporheic zone (HZ) toward the streambed, changing HZ volume from the homogenous case and thus inducing remarkable differences in the flow field with respect to the homogeneous case. We unravel the physical conditions for which the commonly used homogenous field assumption is applicable for quantifying hyporheic processes thus explaining why predictive measures based on a characteristic residence time, like the Damköhler number, are robust in heterogeneous sand bedded streams.

© 2016 The Authors. Published by Elsevier Ltd.
This is an open access article under the CC BY-NC-ND license (http://creativecommons.org/licenses/by-nc-nd/4.0/).

1. Introduction

Hyporheic zone, HZ, is a fundamental component of the stream system (Harvey and Gooseff, 2015; Stanford and Ward, 1993) and exerts an important control in many ecological functions including ecosystem metabolism and bio-geochemical transformations (Boano et al., 2014; Findlay et al., 1993). It is formed by stream water flowing within the streambed sediment (Gooseff, 2010; Thibodeaux and Boyle, 1987), where many biogeochemical reactions occur (Zarnetske et al., 2011; Triska et al., 1993). Hyporheic fluxes modulate the streambed sediment thermal regime (Sawyer et al., 2012; White et al., 1987), its redox conditions (Briggs et al., 2015; Mulholland et al., 1997), its dissolved oxygen concentration (Tonina et al., 2015), nutrients turnover (Beaulieu et al., 2011; Mulholland and DeAngelis, 2000), its habitat quality (Wu, 2000; Baxter and Hauer, 2000) and organism distribution within streambed sediments (Findlay and Sobczak, 2000; Creuzé des Châtelliers and Reygrobellet, 1990). In turn, upwelling waters, those that exit the sediment and rejoin the stream surface water, bring transformed and waste products to the stream water thus affecting surface water quality (Marion and Zaramella, 2008). All these processes are chiefly controlled by the residence time of stream water within the streambed sediment (Zarnetske et al., 2011; Marzadri et al., 2012, Briggs et al., 2014). Streambed morphology modulates hyporheic residence time distribution, henceforth denoted as RTD, such that we identify this distribution as morphologically driven. Recently, Marzadri et al. (2014) showed that emissions of nitrous oxide, N_2O, from streambeds can be predicted with the Damköhler number, which is a dimensionless number defined as the ratio between the median hyporheic residence time, namely τ_{50}, and a biogeochemical characteristic reaction time. A similar approach has been recently applied by Gomez-Velez and Harvey (2014) and Gomez-Velez et al. (2015) to map hyporheic processes at the network scale. Consequently, the quantification of RTD and its statistical moments is of crucial importance at the local bedform scale but also at the network and global scales because of its effects on ecosystem metabolism and climate change through degassing of carbon dioxide and nitrous oxide.

Whereas the effect of streambed morphology on RTD is well understood, although it is predicted with semi-analytical or empirical models using few hydromorphological quantities only for

* Corresponding author. Fax: +12083324425.
E-mail address: dtonina@uidaho.edu (D. Tonina).

http://dx.doi.org/10.1016/j.advwatres.2016.07.009
0309-1708/© 2016 The Authors. Published by Elsevier Ltd. This is an open access article under the CC BY-NC-ND license (http://creativecommons.org/licenses/by-nc-nd/4.0/).

few bedforms (Buffington and Tonina, 2009), other important aspects of streambeds influencing RTD distribution such as the heterogeneity of the hydraulic properties received less attention from the community. The natural heterogeneity of the hydraulic conductivity, K, of the streambed sediment leads to a seemingly erratic distribution of the velocity field in the sediments and generates hyporheic exchange fluxes due to conservation of mass (Tonina, 2012; Ward et al., 2011). The impossibility to characterize the actual spatial variability of K fully renders uncertain both the velocity field and the morphologically-driven RTD. Heterogeneity can manifest at mainly two distinct scales: at the single geological facies (continuous heterogeneity) and at multiple geological facies (categorical heterogeneity). The former is the intrinsic heterogeneity of a porous material due to random changes of porous size and directions (Dagan, 1989). The latter is caused by the arrangement of multiple facies, which form a composite porous media (Riva et al., 2006; Tartakovsky and Winter, 2002). Composite porous media are typically modeled with disjoint blocks, which are internally homogenous. A typical example of categorical heterogeneity in hyporheic zones is that induced by stratified streambeds (Marion et al., 2008; Pryshlak et al., 2015; Gomez-Velez et al., 2014) whereas continuous heterogeneity may be associated with sand-bedded streams below dune-likes bedforms (Hester et al., 2013; Salehin et al., 2004). The latter case is particularly interesting because of the substantial representation of dune-like bedforms in riverine systems (Montgomery and Buffington, 1997). Although previous studies highlighted that heterogeneity at both scales may affect hyporheic flux intensity and residence time (e.g., Marion et al., 2008; Pryshlak et al., 2015; Gomez-Velez et al., 2014; Hester et al., 2013; Salehin et al., 2004; Sawyer and Cardenas, 2009; Cardenas et al., 2004; Zhou et al., 2014), those for continuous heterogeneity did not provide relationship between heterogeneity and uncertainty on RTD and did not address the relationship between the heterogeneous structure of K and the statistical characterization of the RTD at both bedform and reach scales. With the aim of filling this gap and given its importance in global scale processes, we investigate the relationship among the statistical moments of the hyporheic RTD, heterogeneity and spatial correlation scales at the bedform scale and we present a new framework to upscale heterogeneity effects from the bedform to reach. For simplicity, and according to a large body of literature in stochastic hydrogeology (Dagan, 1989; Rubin, 2003), we assume that the spatial distribution of $Y = \ln(K)$ can be represented as a multi-Gaussian random space function model (e.g. continuous heterogeneity). However, we point out that our methodology can be extended to distinct heterogeneity models such as the categorical models (Riva et al., 2006; Tartakovsky and Winter, 2002). The analysis is carried out by making use of a stochastic model of subsurface flow to characterize in probabilistic terms the RTD of stream water within the bedform. Furthermore, we test the performance of the stochastic model in predicting N_2O emissions from hyporheic zone of the subset of LINXII streams (Beaulieu et al., 2011) that are sand-bedded with dune-like bedforms.

2. Methods

Sand-bed rivers are common along the river network. Their dominant bedforms are dune-like features, whose size ranges from small ripples of few centimeters of wavelength and millimeters of amplitude to large dunes of tens of meter wavelength and tenths of meters of amplitude (Montgomery and Buffington, 1997; Ferreira De Silva and Zhang, 1999). These bedforms are mostly composed of fine sediment in the range of sand. In order to investigate the effect of streambed heterogeneity on hyporheic RTD, we consider a statistically stationary spatially heterogeneous K field with uniform porosity equal to 0.3. The log-conductivity field $Y = \ln(K)$ is modeled as a stationary Gaussian random function with mean $<Y>$ and variance σ_Y^2, both constant (uniform). The spatial pattern of Y is controlled by the following exponential covariance function C_Y:

$$C_Y(\boldsymbol{r}) = \sigma_Y^2 \exp\left[-\sqrt{\left(\frac{r_x}{I_{Y,x}}\right)^2 + \left(\frac{r_z}{I_{Y,z}}\right)^2}\right], \tag{1}$$

where $\boldsymbol{r} = (r_x, r_z)$ is the two-point separation distance, with respect to which the covariance function is evaluated and $I_{Y,i}$ (with $i = x, z$) are the integral scales along the longitudinal (horizontal) and transverse (vertical) directions. Common values of heterogeneity degree, epitomized by σ_Y^2, in sand bed rivers range between near 0 (almost a homogenous case) and 0.6 (low heterogeneity), (Hess et al., 1992 and reference within) and may be larger above unity in case of mixed sand and fine gravel (Zhou et al., 2014). Stratification, which is manifested with layers with longest axis along the streambed slope direction (mainly horizontal layers), causes statistical K-field anisotropy, which can be measured with the ratio between the integral scales along the horizontal $I_{Y,x}$ and vertical $I_{Y,z}$ directions (i.e. $f = I_{Y,x}/I_{Y,z}$). Values for f may range from $f = 1$ (isotropic case) to $f \approx 18$ (strong anisotropy) (Kessler et al., 2013; Ritzi et al., 2004).

To quantify the impact of the randomness of Y on the statistical moments of the RTD, we used the Monte Carlo (MC) approach to generate multiple realizations of the heterogeneous K-field obeying the spatial correlation structure (1). The K-fields are generated by using Hydro_GEN (Bellin and Rubin, 1996) and specifying values for $I_{Y,x}$, $I_{Y,z}$, $<Y>$ and σ_Y^2. As in Hester et al. (2013), we model the hyporheic flow in one dune with 0.915 m wavelength, λ, and 0.138 m amplitude, Δ, with MODFLOW (Harbaugh, 2005) on a numerical domain represented by a 2D grid with 0.915 m in the horizontal extent and 1.14 m in the vertical extent with a 0.0025 m square cell size. The model simulates a steady state seepage flow in which: i) the pressure head boundary condition of Run 6 of the laboratory experiments conducted by Shen et al. (1990) is imposed at the water sediment interface and ii) a gaining flow condition is imposed at the lower boundary domain (constant groundwater flux: $q_{GW} = 3 \times 10^{-3}$ m/d). A number of particles ($N = 366$, i.e. large enough to stabilize the RTD moments) are released in the downwelling zone and tracked by MODPATH until they exit from the upwelling zone. We calculate the first three flux-weighted moments (mean, variance and skewness) of $\tau_i^{(j)}$, which is the residence time of a particle released at the ith downwelling position in the jth realization due to the streambed morphology:

$$\begin{aligned}
\bar{\tau}^{(j)} &= \frac{\sum_{i=1}^{N} \tau_i^{(j)}\, q_i^{(j)}\, \Delta A_i}{\sum_{i=1}^{N} q_i^{(j)}\, \Delta A_i}, \\
\sigma_\tau^{2(j)} &= \frac{\sum_{i=1}^{N} \left(\tau_i^{(j)} - \bar{\tau}^{(j)}\right)^2 q_i^{(j)} \Delta A_i}{\sum_{i=1}^{N} q_i^{(j)}\, \Delta A_i}, \\
\gamma_1^{(j)} &= \frac{\sum_{i=1}^{N} \left(\frac{\tau_i^{(j)} - \bar{\tau}^{(j)}}{\sigma_\tau}\right)^3 q_i^{(j)}\, \Delta A_i}{\sum_{i=1}^{N} q_i^{(j)}\, \Delta A_i}
\end{aligned} \tag{2}$$

where $q_i^{(j)}$ is the specific water discharge normal to the downwelling areas at the ith position where the particle enters the downwelling areas in the jth MC realization, and ΔA_i is the cross-sectional area of the streamtube originating from this location.

These moments coincide with the temporal moments of the BTC recorded at the upwelling area for a flux proportional injection of solute through the downwelling area, which is consistent with the hypothesis of in-stream well-mixed solute concentration. We also evaluate the median $\tau_{50}^{(j)}$. In addition, we calculate the

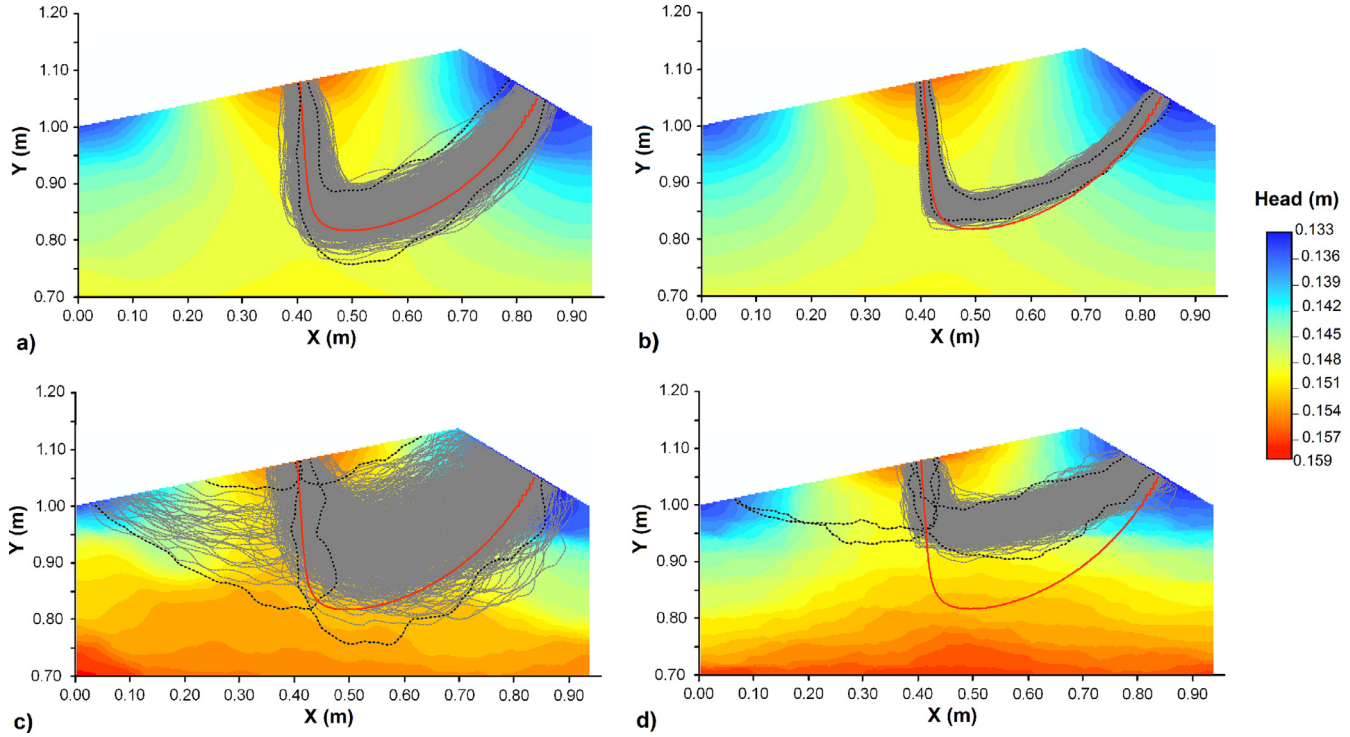

Fig. 1. Head distribution for *j*th MC realization to show the head variability due to heterogeneity and the deepest streamlines obtained in the homogeneous case (red line) and in each of the 1000 MC realizations of the heterogeneous case (gray lines) with upper and lower bounds of variability for the deepest flow lines (dashed black lines). Results are for (a) $\sigma^2_Y=0.3$ and $f=1$ (b) $\sigma^2_Y=0.3$ and $f=18$ (c) $\sigma^2_Y=1.5$ and $f=1$ (d) $\sigma^2_Y=1.5$ and $f=18$. (For interpretation of the references to color in this figure legend, the reader is referred to the web version of this article.)

ensemble mean of the above moments as

$$\langle\bar{\tau}\rangle = \frac{\sum_j^{NMC}\bar{\tau}^{(j)}}{NMC},\ \langle\sigma_\tau^2\rangle = \frac{\sum_j^{NMC}\sigma_\tau^{2(j)}}{NMC},$$
$$\langle\gamma_1\rangle = \frac{\sum_j^{NMC}\gamma_1^{(j)}}{NMC},\ \langle\tau_{50}\rangle = \frac{\sum_j^{NMC}\tau_{50}^{(j)}}{NMC} \quad (3)$$

where *NMC* is the number of MC realizations. We achieved statistical convergence with 800 MC realizations and our results are reported with a total of *NMC*=1000. We also quantify the ensemble mean of the (spatially) mean downwelling flux, $\langle\bar{q}\rangle$ and of the flow line length for each *i*th downwelling position:

$$\langle\bar{q}\rangle = \frac{\sum_j^{NMC}\bar{q}_i^{(j)}}{NMC};\ \langle F_{l,i}\rangle = \frac{\sum_j^{NMC}F_{l,i}^{(j)}}{NMC} \quad (4)$$

where $\bar{q}^{(j)}=\sum_{i=1}^{N}q_i^{(j)}\ \Delta A_i/\sum_{i=1}^{N}\Delta A_i$ is the mean downwelling flux and $F_{l,i}$ is the length of the streamline originating in the *i*th position for each MC realization. Dimensionless emissions of N_2O, $F^*_{N_2O}$, can be computed with the expression (Marzadri et al., 2014):

$$F^*_{N_2O} = a\ Da_0^m, \quad (5)$$

where *a* and *m* are coefficients equal to $1.14\cdot10^{-7}$ and 0.23 respectively, The dimensionless Damköhler number is quantified as, $Da_o=\tau_{50}\ /\ \tau_{lim}$, with τ_{lim} the time at which dissolved oxygen concentrations reach anoxic conditions within the hyporheic zone. Consequently, $F^*_{N_2O}$ moments can be quantified from the probability distribution of $\tau_{50}^{(j)}$, $p(\tau_{50})$, such that the expected flux is:

$$\langle F^*_{N_2O}\rangle = \int_0^\infty F^*_{N_2O}dF^*_{N_2O} = \frac{a}{\tau_{lim}^m}\int_0^\infty \tau_{50}^m\ p(\tau_{50})d\tau_{50}, \quad (6)$$

To quantify Da_o, we used the values of τ_{lim} reported in the work of Marzadri et al. (2014) and hydromorphological characteristics of the LINXII streams to estimate τ_{50} with only sand beds and dune morphology.

We designed a set of simulations where we ranged σ_Y^2 from 0 to 2.1 with incremental steps of 0.3. We fix $I_{Y,z}=0.05$ m and varied $I_{Y,x}$ from 0.05, 0.10, 0.20, 0.50, 0.70 and 0.90 m such that $\rho=100$ $I_{Y,x}/\lambda$ ranged between 5.5 and 98.3%. In this work, we opted to change the anisotropy ratio *f* by varying $I_{Y,x}$, while keeping $I_{Y,z}$ fixed, because dunes are formed by hydrodynamic sorting of material occurring chiefly in vertical direction, thereby stratification is constrained by the relatively small height of the dune with respect to its wavelength (e.g., Miall, 2012 Fig. 5.18). Notice that the largest value adopted for $I_{Y,x}$, which leads to $f=18$ in the present work, is consistent with the values observed in sandy aquifers (Rubin, 2003).

3. Results and discussion

Heterogeneity of the *K*-field causes the trajectories (gray solid lines, Fig. 1) of the deepest flow paths not only to alternate between downstream and upstream hyporheic flow cells, though in the majority of the MC realizations they remain in the downstream cell, but also their depth to vary among MC realizations (Fig. 1). Additionally the position where the deepest flow line originates varies among realizations around that of the homogeneous case. Heterogeneity increases the tortuosity of the flow lines and simultaneously tends to keep the flow paths closer to the streambed surface resulting in shallower hyporheic zones when compared to the homogenous case (c.f. red line and deeper dashed black line Fig. 1). This effect is augmented for large heterogeneity as observed in groundwater studies (de Barros et al., 2012; Cirpka et al., 2011). The net effect of the heterogeneity is a compression of the HZ near the streambed surface. It also increases the length of the short flow lines due to tortuosity and reduces medium to long flow lines due to compression (Fig. 2b). Heterogeneity also switches certain upwelling to downwelling zone as shown by the presence of short flow lines for the heterogeneous case where there was no streamlines for the homogenous case as shown by the symbols along the

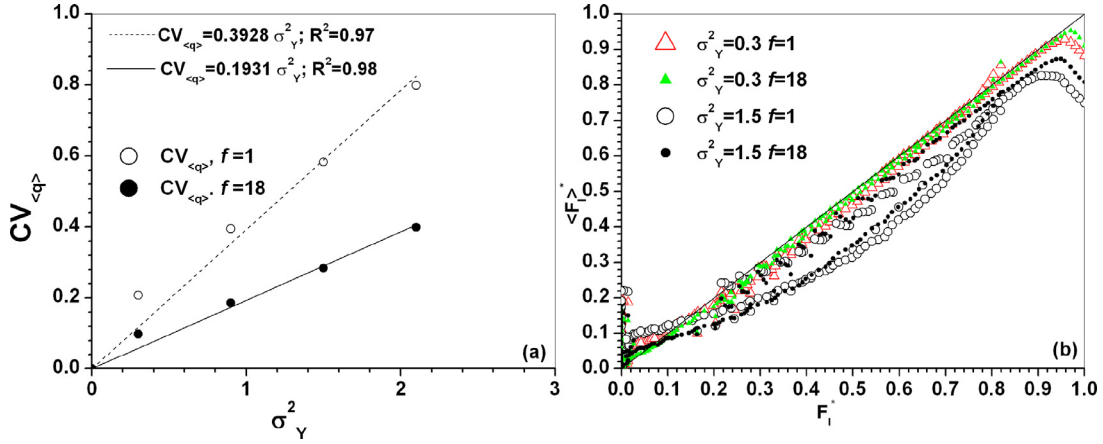

Fig. 2. Coefficient of variation of the mean downwelling flux (a) and comparison between ensemble length of the flow path originating in a given downwelling position and its homogenous counterpart (b). Flow line length has been normalized by the longest flow line of the homogenous case.

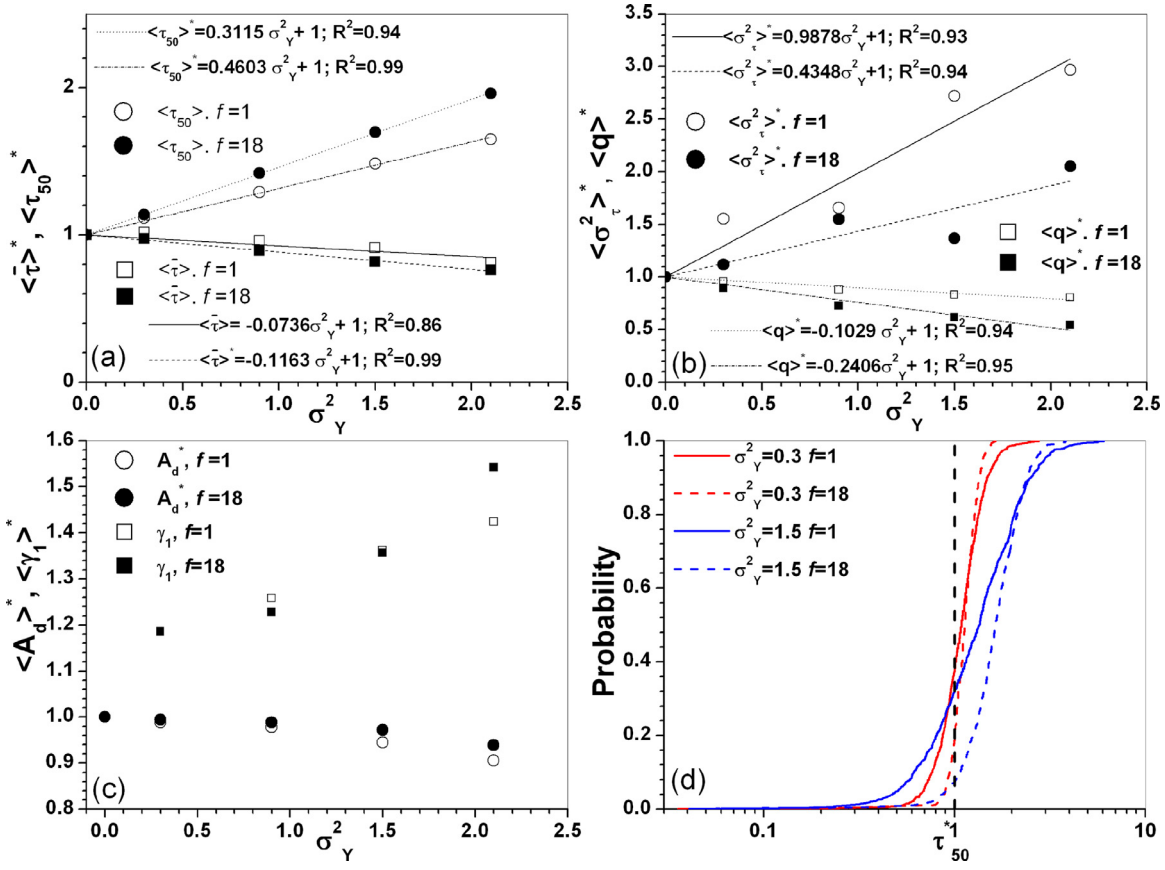

Fig. 3. Expected values over all the MC realizations of the dimensionless: (a) mean $\langle\bar{\tau}\rangle^*$, median ($\langle\tau_{50}\rangle^*$); (b) variance ($\sigma^{2*}_\tau$), downwelling flux ($\langle q\rangle^*$) and (c) skewness ($\gamma_1{}^*$)) of the hyporheic RTD at the bedform scale and the extent of the dimensionless downwelling area ($\langle A_d\rangle^*$); and (d) distribution of dimensionless median residence time, $\tau_{50}^{(j)*}$, over the 1000 MC realizations for $\sigma^2{}_Y=0.3$ and 1.5 and $f=1$ and 18. All quantities are normalized with their homogenous case values.

ordinate axis in Fig. 2b. Notice that the depth of the HZ varies substantially among realizations (Fig. 1 black dashed lines which bound the collection of deepest flow lines identified in each MC realization).

This uncertainty on the HZ vertical extent is reduced by sediment anisotropy, which focuses the streamlines among realizations. Both heterogeneity and sediment anisotropy decrease the ensemble mean of the spatially averaged downwelling flux, resulting in a reduction of the average exchange between stream and sediment (Fig. 3b). However, heterogeneity increases exchange flux variability among realizations (i.e. $\bar{q}^{(j)}$ for j=1, …, NMC) whereas sediment anisotropy attenuates this variability by focusing the flow lines (Fig. 2a). Similarly, the ensemble downwelling area decreases with heterogeneity to almost 10% for high heterogeneity and isotropic sediment, suggesting that the net effect of heterogeneity is to switch most location as upwelling than downwelling (Fig. 3c).

The effect of the statistical anisotropy of the hydraulic conductivity on the RTD are noticeable up to $f=10$. For values $f>10$, the RTD moment changes are small. The maximum differences between $f=10$ and $f=18$ are 6%, 8% and 23% for $\langle\bar{\tau}\rangle$, $\langle\tau_{50}\rangle$ and $\langle\sigma^2_\tau\rangle$, respectively, regardless of $\sigma^2{}_Y$. We attribute this behavior to the

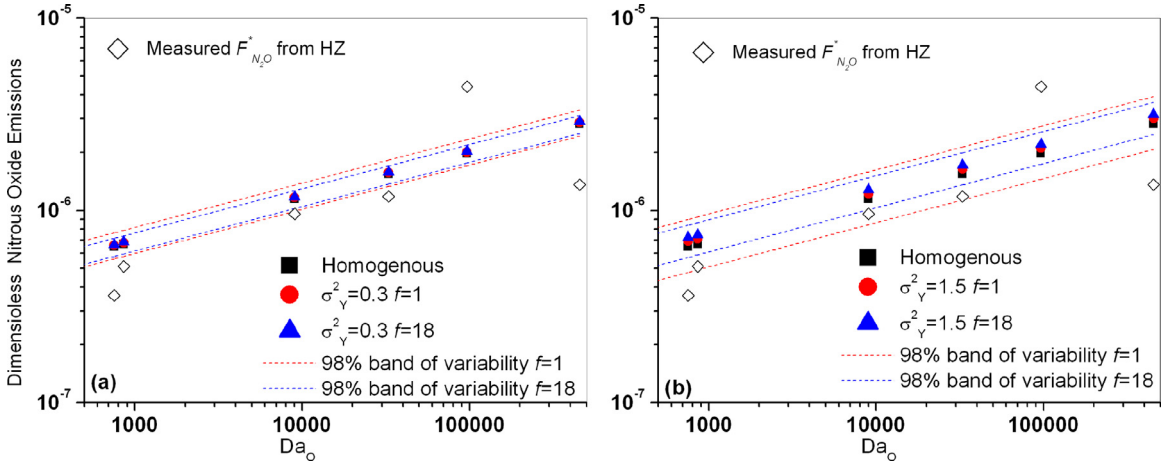

Fig. 4. Nitrous oxide emissions (dimensionless as defined by Marzadri et al. (2014)) as a function of the Damköhler number, Da_o, for (a) low and (b) high heterogeneity.

fact that the horizontal integral scale $I_{Y,x}$ corresponds to 50% of the dune length (ρ=50%). Although, at the present stage, the effects of f and ρ are not fully disentangled, our results suggest that the statistical anisotropy reaches its maximum effect on RTD (and consequently larger f may add negligible changes in RTD) when ρ is approximately equal to 50% since it effectively alters the flow field as it were a layer extending the entire dune length. This is due to the fact that hyporheic exchange is a flow cell with half flow downwelling and the other upwelling such that for $\rho > 50\%$, streamlines cross strata nearly homogeneous in horizontal direction and heterogeneous in the vertical one. Notice that, in natural geological formations $I_{Y,x}$ and $I_{Y,z}$ are not independent quantities, since they are related to the depositional process that created the dune (and therefore to ρ). Therefore, we suggest that disentangling the effects of f from that of ρ on the RTD requires additional research on the relationship among streambed geological formation, bedform size and heterogeneity structure.

An important consequence of streamline compression is that the streamline originating from a given position in the downwelling area deviates from the streamline originating from the same position in a homogeneous domain instead of oscillating around it as in the case of uniform mean velocity analyzed in stochastic groundwater literature (Dagan et al., 1992). Note that this result differs from the first-order analysis in a uniform mean velocity field, which leads to a constant $\langle\bar{\tau}\rangle$ (Dagan et al., 1992) (at least for small heterogeneity in the permeability field). Conversely from the groundwater literature, where most studies focus on uniform-in-the-mean flow conditions and convergent flows, flow fields within the HZ is strongly affected by boundary effects. These boundary effects, together with stream-bed heterogeneity, cause $\langle\bar{\tau}\rangle$ to decrease with respect to the homogeneous case (Fig. 3a).

All moments of RTD deviate increasingly from those of the homogeneous case, as σ^2_Y increases. Instead, in the homogenous case, the moments reflect flow non-uniformity dictated by streambed morphology (only morphologically driven RTD), rather than heterogeneity in the hydraulic conductivity of the alluvium. However, for weak heterogeneity (i.e., $\sigma^2_Y < 0.6$) the difference is relatively small for all moments and the effect of morphology prevails. Instead at $\sigma^2_Y = 0.9$ and $f=1$, the spatial mean ($\langle\bar{\tau}\rangle$) decreases by 4% and variance ($\langle\sigma^2_\tau\rangle$) increases 65%, with respect to the homogeneous case, while for $\sigma^2_Y = 2.1$ $\langle\bar{\tau}\rangle$ decreases by 19% and σ^2_τ increases 197%, respectively, thereby similar the effect of streambed morphology (Stonedahl et al., 2013; Stonedahl et al., 2010). This suggests that high heterogeneity may have the same effect on RTD uncertainty of dune-like bedform size variability along a reach (Stonedahl et al., 2013; Stonedahl et al., 2010). Statistical anisotropy reduces the difference between homogenous and heterogeneous cases because of the additional flow compression effect introduced by layering (see also Figs. 1 and 2b). The effect of heterogeneity and anisotropy on the median residence time is also small at low heterogeneity 10% for $\sigma^2_Y = 0.3$ and increases to 64% for high $\sigma^2_Y = 2.1$. The median residence time is a key index for predicting N_2O emissions from the hyporheic zone as proposed by Marzadri et al. (2014). Consequently, scaling of hyporheic processes through the Damköhler number computed with reference to $\langle\tau_{50}\rangle$ are expected to be robust, because it takes into account the combined effect of streambed morphology and alluvium heterogeneity. The variability of τ_{50} among the MC realizations is a source of uncertainty of this scaling, which can be quantified statistically by observing that frequency distribution of τ_{50} follows a Gamma distribution, (statistically significant for Kolmogorov-Smirnov D < critical value 0.042 with $\alpha = 0.05$), fully characterized by $\langle\tau_{50}\rangle$ and $\sigma^2_{\tau_{50}}$. Similar considerations can be made for other hyporheic processes that depend upon transport dynamics such as energy exchange, conservative and non-conservative solute retention.

The red and blue dashed lines in Fig. 4 show the 98% confidence intervals (by setting the probability 1% and the 99% in Fig. 3d and reading the τ_{50} from its distribution) on the emissions due to the variability of τ_{50} among the MC realizations for the isotropic ($f=1$) and highly anisotropic ($f=18$) cases, respectively. No appreciable differences are observed between emissions computed in the homogeneous case and the ensemble mean of those computed in the heterogeneous case (Eq. 6) while uncertainty partially explains the differences between the computed and measured (open diamonds Fig. 4) emissions (see the uncertainty bounds).

We interpret these findings to suggest a novel physically driven conceptual approach to interpret heterogeneity at the reach scale. It is important to notice that the streambed can contain hundreds of dunes/ripples within a stream reach (10^2 channel widths) or stream segment (10^3 channel widths). This indicates that we could exchange space with ensemble average (ergodic conditions, supposing small morphological variability among dunes (Stonedahl et al., 2013; Stonedahl et al., 2010)) as long as there is a sufficient number of dune-like bedforms, each taking a different realization of the K-field. In other words, we argue that the mean RTD over the different dunes along a reach will resemble that of the ensemble over all the realizations of the K-field, as the system becomes ergodic. This implies that $\langle\tau_{50}\rangle$ coincides with the median residence time of the hyporheic flow at the reach scale of similar dune shape and size. This solution could be potentially applicable in case of variable dune-like bedform sizes by using the spatially averaged dune-like bedform size as shown by Stonedahl et al. (2010), who demonstrated that spatially averaged dune-like

bedform size provides good approximation of the hyporheic RTD at the reach scale. Relationships like those provided in Fig. 3 can then be used to quantify the statistical moments of the expected RTD at the reach scale. Consequently, we suggest that the variability of the RTD due to sediment heterogeneity expresses two important concepts. First, it is the uncertainty due to heterogeneity of the hydraulic conductivity that we can expect at the bedform scale, which may explain most of the difference between model results and measurements, as shown in Fig. 4. Secondly, it expresses the spatial variability of hyporheic processes at the reach scale, where each dune-like bedform of similar size and shape within a reach will have their own flow field modulated by the heterogeneity. Consequently, as an effect of alluvium heterogeneity, hyporheic measurements collected at one bedform may not be representative of the entire reach. This leads to the conclusion that the interpretation of the effect of heterogeneity on hyporheic exchange varies with the length scale from single to multiple dunes, at which the processes are observed. However, a statistical framework as that used in the letter provides the means to quantify the uncertainty.

4. Conclusions

Our analysis reveals that heterogeneity causes a compression effect of the hyporheic zone and a reduction of ensemble hyporheic mean exchange. Whereas heterogeneity increases tortuosity of the flow lines, thus increasing residence time of flow paths of short lengths, it reduces that of the long residence times with respect to the homogeneous case because of compression of the HZ. However, the net results of heterogeneity is to decrease the mean but increase the median, variance and skewness of the hyporheic flux-weighted RTD. The reduction of the mean is due to the progressive compression of streamlines within a thin near-bed layer, which does not contrast the increase of the other moments with σ_Y^2, which being central moments are chiefly controlled by heterogeneity. We suggest that the ensemble statistics can be interpreted as the hyporheic zone RTD associated to the reach scale, because over a long reach different dune-like bedforms can be sampled by different solute particles, thereby introducing a sort of operational ergodicity. Heterogeneity also causes some zones to switch between upwelling and downwelling from the homogeneous case. The extension and number of these switching zones increase with heterogeneity and the net effect is to reduce the extent of the downwelling zone. Heterogeneity also has a net effect to reduce hyporheic exchange fluxes and consequently may have important influence on reactive transport (i.e. nutrient reaction rates).

Through a systematic investigation, our analysis supports the use of the homogenous hydraulic conductivity assumption for low heterogeneity, i.e. $\sigma_Y^2 < 0.6$, typically encountered in sand-bedded streams regardless of anisotropy up to a value of $f=18$. Consequently, reach scale approaches based on the statistical moments of the hyporheic residence time, such as the Damköhler number, are robust metrics with respect to uncertainty due to heterogeneity of the streambed sediment for sand bedded rivers. Furthermore, we provide a set of solutions for the RTD moments for medium high heterogeneity. As an outlook into the future, the effect of the near surface sediment heterogeneity of gravel bed rivers on hyporheic process may also be analyzed using our proposed framework.

Acknowledgment

AB acknowledges the support by the European Union FP7 Collaborative Research Project GLOBAQUA (Managing the effects of multiple stressors on aquatic ecosystems under water scarcity, grant 603629). This research was also partially funded by the National Science Foundation grant 1344602. Any opinions, conclusions, or recommendations expressed in this letter are those of the authors and do not necessarily reflect the views of the supporting agencies.

We thank the critical and constructive comments of three anonymous reviewers and the Editor.

References

Baxter, C.V., Hauer, R.F., 2000. Geomorphology, hyporheic exchange, and selection of spawning habitat by bull trout (*Salvelinus confluentus*). Can. J. Fish Aquat. Sci. 57, 1470–1481.
Beaulieu, J.J., Tank, J.L., Hamilton, S.K., Wollheim, W.M., Hall, R.O.J., Mulholland, P.J., et al., 2011. Nitrous oxide emission from denitrification in stream and river networks. Proc. Nat. Acad. Sci. U.S.A. 108, 214–219.
Bellin, A., Rubin, Y., 1996. HYDRO_GEN: a spatially distributed random field generator for correlated properties. Stochastic Hydrol. Hydraul. 10, 253278.
Boano, F., Harvey, J.W., Marion, A., Packman, A.I., Revelli, R., Ridolfi, L., et al., 2014. Hyporheic flow and transport processes: mechanisms, models, and biogeochemical implications. Rev. Geophys. 52, 603–679.
Briggs, M.A., Day-Lewis, F.D., Zarnetske, J.P., Harvey, J.W., 2015. A physical explanation for the development of redox microzones in hyporheic flow. Geophys. Res. Lett. 42.
Briggs, M.A., Lautz, L., Hare, D.K., 2014. Residence time control on hot moments of net nitrate production and uptake in the hyporheic zone. Hydrol. Process. 28, 3741–3751.
Buffington, J.M., Tonina, D., 2009. Hyporheic exchange in mountain rivers II: effects of channel morphology on mechanics, scales, and rates of exchange. Geography Compass 3, 1038–1062.
Cardenas, M.B., Wilson, J.F., Zlotnik, V.A., 2004. Impact of heterogeneity, bed forms, and stream curvature on subchannel hyporheic exchange. Water Resour. Res. 40.
Cirpka, O.A., de Barros, F.P.J., Chiogna, G., Rolle, M., Nowak, W., 2011. Stochastic flux-related analysis of transverse mixing in two-dimensional heterogeneous porous media. Water Resour. Res. 47, W06515.
Creuzé des Châtelliers, M., Reygrobellet, J.L., 1990. Interactions between geomorphological processes and benthic and hyporheic communities: first results on a by–passed canal of the French Upper Rhone River. Regul. Rivers 5, 139–158.
Dagan, G., 1989. Flow and Transport in Porous Formation. Springer-Verlag.
Dagan, G., Cvetkovic, V., Shapiro, A.M., 1992. A solute flux approach to transport in heterogeneous formations: 1. The general framework. Water Resour. Res. 28, 1369–1376.
de Barros, F.P.J., Dentz, M., Koch, J., Nowak, W., 2012. Flow topology and scalar mixing in spatially heterogeneous flow fields. Geophys. Res. Lett. 39, L08404.
Ferreira De Silva, A.M., Zhang, Y., 1999. On the steepness of dunes and determination of alluvial stream friction factor. In: IAHR (Ed.), XXVIII IAHR Congress. IAHR, Graz, Austria, p. 7.
Findlay, S., Sobczak, W.V., 2000. Microbial communities in hyporheic sediments. In: Jones, J.B., Mulholland, P.J. (Eds.), Streams and Ground Waters. Academic Press, San Diego, Calif., pp. 287–306.
Findlay, S., Strayer, W., Goumbala, C., Gould, K., 1993. Metabolism of streamwater dissolved organic carbon in the shallow hyporheic zone. Limnol. Oceanogr. 38, 1493–1499.
Gomez-Velez, J.D., Harvey, J.W., 2014. A hydrogeomorphic river network model predicts where and why hyporheic exchange is important in large basins. Geophys. Res. Lett. 41, 6403–6412.
Gomez-Velez, J.D., Harvey, J.W., Cardenas, B.M., Kiel, B., 2015. Denitrification in the Mississippi River network controlled by flow through river bedforms. Nature Geoscience 8, 941–945.
Gomez-Velez, J.D., Krause, S., Wilson, J.L., 2014. Effect of low-permeability layers on spatial patterns of hyporheic exchange and groundwater upwelling. Water Resour. Res. 50, 5196–5215.
Gooseff, M.N., 2010. Defining hyporheic zones- advancing our conceptual and operational definitions of where stream water and groundwater meet. Geography. Compass. 4, 945–955.
Harbaugh, A.W., 2005. MODFLOW-2005, the U.S. geological survey modular ground-water model—the ground-water flow process U.S. Geological Survey, Reston, Va.
Harvey, J.W., Gooseff, M.N., 2015. River corridor science: hydrologic exchange and ecological consequences from bedforms to basins. Water Resour. Res. 51, 6893–6922.
Hess, K.M., Wolf, S.H., Celia, M.A., 1992. Large-scale natural gradient tracer test in sand and gravel, cape cod, Massachusetts: 3 Hydraulic conductivity variability and calculated macrodispersivities. Water Resour. Res. 28, 2011–2027.
Hester, E.T., Young, K.I., Widdowson, M.A., 2013. Mixing of surface and groundwater induced by riverbed dunes: implications for hyporheic zone definitions and pollutant reactions. Water Resour. Res. 49, 5221–5237.
Kessler, T.C., Comunian, A., Oriani, F., Renard, P., Nilsson, B., Klint, K.E., et al., 2013. Modeling fine-scale geological heterogeneity—examples of sand lenses in tills. Groundwater 51, 692–705.
Marion, A., Packman, A.I., Zaramella, M., 2008. A Bottacin-Busolin. Hyporheic flows in stratified beds. Water Resour. Res 44, W09433.
Marion, A., Zaramella, M., 2008. A Bottacin-Busolin. solute transport in rivers with multiple storage zones: the STIR model. Water Resour. Res. 44, W10406.

Marzadri, A., Tonina, D., Bellin, A., 2012. Morphodynamic controls on redox conditions and on nitrogen dynamics within the hyporheic zone: application to gravel bed rivers with alternate-bar morphology. J. Geophys. Res. 117.
Marzadri, A., Tonina, D., Bellin, A., Tank, J.L., 2014. A hydrologic model demonstrates nitrous oxide emissions depend on streambed morphology. Geophys. Res. Lett. 41, 5484–5491.
Miall, A.D., 2012. The Geology of Fluvial Deposits: Sedimentary Facies, Basin Analysis, and Petroleum Geology. Springer-Verlag, Berlin Heidelberg.
Montgomery, D.R., Buffington, J.M., 1997. Channel-reach morphology in mountain drainage basins. Geol. Soc. Am. Bull. 109, 596–611.
Mulholland, P.J., DeAngelis, D.L., 2000. Surface-subsurface exchange and nutrient spiraling. In: Jones, J.B., Mulholland, P.J. (Eds.), Streams and Ground Waters. Academic Press, San Diego, Calif, pp. 149–168.
Mulholland, P.J., Marzorf, E.R., Webster, J.R., Hart, D.D., Hendricks, S.P., 1997. Evidence that hyporheic zones increase heterotrophic metabolism and phosphorus uptake in forest streams. Limnol. Oceanogr. 42, 443–451.
Pryshlak, T.T., Sawyer, A.H., Stonedahl, S.H., Soltanian, M.R., 2015. Multiscale hyporheic exchange through strongly heterogeneous sediments. Water Resour. Res..
Ritzi, R.W., Dai, Z., Dominic, D.F., Rubin, Y.N., 2004. Spatial correlation of permeability in cross-stratified sediment with hierarchical architecture. Water Resour. Res. 40, W03513.
Riva, M., Guadagnini, L., Guadagnini, A., Ptak, T., Martac, E., 2006. Probabilistic study of well capture zones distribution at the Lauswiesen field site. J. Contam. Hydrol. 88, 92–118.
Rubin, Y., 2003. Applied Stochastic Hydrology. Oxford University Press, New York, NY.
Salehin, M., Packman, A.I., Paradis, M., 2004. Hyporheic exchange with heterogeneous streambeds: laboratory experiments and modeling. Water Resour. Res. 40.
Sawyer, A.H., Cardenas, B.M., 2009. Hyporheic flow and residence time distributions in heterogeneous cross-bedded sediment. Water Resour. Res. 45, W08406.
Sawyer, A.H., Cardenas, B.M., Buttles, J., 2012. Hyporheic temperature dynamics and heat exchange near channel-spanning logs. Water Resour. Res. 48, W01529.
Shen, H.V., Fehlman, H.M., Mendoza, C., 1990. Bed form resistances in open channel flows. J Hydraul. Eng. 116, 799–815.
Stanford, J.A., Ward, J.V., 1993. An ecosystem perspective of alluvial rivers: connectivity and the hyporheic corridor. J. North Am. Benthol. Soc. 12, 48–60.
Stonedahl, S.H., Harvey, J.W., Packman, A.I., 2013. Interaction between hyporheic flow produced by stream meanders, bars and dunes. Water Resour. Res. 49, 5450–5461.
Stonedahl, S.H., Harvey, J.W., Wörman, A., Salehin, M., Packman, A.I., 2010. A multi--scale model for integrating hyporheic exchange from ripples to meanders. Water Resour. Res. 46, W12539.
Tartakovsky, D.M., Winter, C.L., 2002. Groundwater flow in heterogeneous composite aquifers. Water Resour. Res. 38.
Thibodeaux, L.J., Boyle, J.D., 1987. Bedform-generated convective transport in bottom sediment. Nature 325, 341–343.
Tonina, D., Marzadri, A., Bellin, A., 2015. Benthic uptake rate due to hyporheic exchange: The effects of streambed morphology for constant and sinusoidally varying nutrient loads. Water 7, 398–419.
Tonina, D., 2012. Surface water and streambed sediment interaction: The hyporheic exchange. In: Gualtieri, C., Mihailović, D.T. (Eds.), Fluid Mechanics of Environmental Interfaces. CRC Press, Taylor & Francis Group, London, UK, pp. 255–294.
Triska, F.J., Duff, J.H., Avanzino, R.J., 1993. The role of water exchange between a stream channel and its hyporheic zone in nitrogen cycling at the terrestrial-aquatic interface. Hydrobiologia 251, 167–184.
Ward, A.S., Gooseff, M.N., Johnson, P.A., 2011. How can subsurface modifications to hydraulic conductivity be designed as stream restoration structures? Analysis of vaux's conceptual models to enhance hyporheic exchange. Water Resour. Res. 47, W09418.
White, D.F., Elzinga, C.H., Hendricks, S.P., 1987. Temperature patterns within the hyporheic zone of a northern Michigan river. J. North Am. Benthol. Soc. 62, 85–91.
Wu, F.-C., 2000. Modeling embryo survival affected by sediment deposition into salmonid spawning gravels: Application to flushing flow prescriptions.. Water Resour. Res. 36, 1595–1603.
Zarnetske, J.P., Haggerty, R., Wondzell, S.M., Baker, M.A., 2011. Dynamics of nitrate production and removal as a function of residence time in the hyporheic zone. J. Geophys. Res. 116, G01025.
Zhou, Y., Ritzi, R.W., Soltanian, M.R., Dominic, D.F., 2014. The influence of streambed heterogeneity on hyporheic flow in gravelly rivers. Groundwater 52, 206–216.